Four

Liquid Flat-Plate Collectors

A brief description of the liquid flat-plate collector has been given in Sec. 2.1, and its varied applications have been described in Sec. 2.2. These include water heating, space heating and cooling, and low-temperature cycles for power generation.

4.1 GENERAL

The basic parts that make up a conventional liquid flat-plate collector are (i) the absorber plate, (ii) the tubes fixed to the absorber plate through which the liquid to be heated flows, (iii) the transparent covers, and (iv) the insulated container. The main advantage of a flat-plate collector is that it utilizes both the beam and diffuse components of the solar radiation. In addition, because of its simple stationary design, it requires little maintenance. Its principal disadvantage is that because of the absence of optical concentration, the area from which heat is lost is large. As a result, the collection efficiency is generally low.

The liquid heated is generally water. However, sometimes mixtures of water and ethylene glycol are used if ambient temperatures below 0°C are likely to be encountered. The absorber plate is usually made from a metal sheet ranging in thickness from 0.2 to 1 mm, while the

tubes, which are also of metal, range in diameter from 1 to 1.5 cm. They are soldered, brazed, welded or pressure bonded to the bottom of the absorber plate with the pitch ranging from 5 to 12 cm. In some designs, the tubes are bonded to the top or are in-line and integral with the absorber plate. The metal most commonly used, both for the absorber plate and the tubes, is copper. However, in India, because of the shortage of copper, other absorber plate-tube combinations have been successfully developed. These include aluminium sheets fixed to copper or galvanized steel tubes with a pressure bond, mild steel or galvanized steel sheets with galvanized steel tubes, and stainless steel sheets with built-in channels. The header pipes, which lead the water in and out of the collector and distribute it to the tubes, are made of the same metal as the tubes and are of slightly larger diameters (2 to 2.5 cm).

Plain or toughened glass of 4 or 5 mm thickness is the most favoured material for the transparent covers. The usual practice is to have one or two covers with spacings ranging from 1.5 to 3 cm.

The bottom and sides are usually insulated by mineral wool, rock wool or glass wool with a covering of aluminium foil and has a thickness ranging from 2.5 to 8 cm. The whole assembly is contained within a box which is tilted at a suitable angle. The collector box may be made of aluminium, steel sheet, or fibre glass.

The face areas of most commercially available collectors are around 2 m^2, with the length (along the sloping direction) being usually larger than the width.

More details of the components used in collectors are given in IS 12933 (Part 2)*.

In the last few years, the use of plastic materials for the absorber plate, the tubes as well as the covers has increased. This is particularly true for applications involving lower temperatures up to 60 or 70°C. Initially plastics were not used because they degraded on exposure to sunlight. They also have low thermal conductivities and high coefficients of expansion as compared to metals. However, recent advances in polymer technology have resulted in the development of suitable plastic materials which can withstand long exposures to sunlight. Plastics have the advantages of being light in weight and easy to manufacture. They also cost less and require less energy input for their manufacture than metals like copper and aluminium. However, it has to be remembered that they generally originate from fossil fuels. As the volume of production of flat-plate collectors increases, the above considerations of energy input and raw material origin will become increasingly important.

The present rate of production of liquid flat-plate collectors in the world, as well as in India, is low. However, it is increasing rapidly. About 200 000 m^2 have been installed in India in the 1980's. The typical cost of a good quality collector is about Rs 3500 per square metre. Installed costs of systems are usually about $1\frac{1}{2}$ times the above cost, since they include the cost of erection, piping and accessories.

4.2 PERFORMANCE ANALYSIS

We will now take up for detailed consideration the performance analysis of a liquid flat-plate collector. The analysis will first be done for a steady state situation* in which the liquid is flowing through tubes bonded on the under-side of the absorber plate. Later on, the results for other types of flat-plate collectors will be given and transient effects will be considered.

An energy balance on the absorber plate yields the following equation for a steady state

$$q_u = A_p S - q_l \tag{4.1}$$

in which

q_u = useful heat gain, i.e. the rate of heat transfer to the working fluid,

S = incident solar flux absorbed in the absorber plate,

A_p = area of the absorber plate,

q_l = rate at which heat is lost by convection and re-radiation from the top, and by conduction and convection from the bottom and sides.

From Sec. 3.7, the flux incident on the top cover of the collector is given by Eq. (3.33)

$$I_T = I_b r_b + I_d r_d + (I_b + I_d) r_r$$

Each of the terms in the above equation is multiplied by a term called the transmissivity-absorptivity product $(\tau\alpha)$ in order to determine the flux S absorbed in the absorber plate. Thus,

$$S = I_b r_b (\tau\alpha)_b + \{I_d r_d + (I_b + I_d) r_r\} (\tau\alpha)_d \tag{4.2}$$

However, quasi-steady

in which,

τ = transmissivity of the glass cover system, the ratio of the solar radiation coming through after reflection at the glass-air interfaces and absorption in the glass to the radiation incident on the glass cover system,

α = absorptivity of the absorber plate,

$(\tau\alpha)_b$ = transmissivity-absorptivity product for beam radiation falling on the collector (defined in Sec. 4.4),

$(\tau\alpha)_d$ = transmissivity-absorptivity product for diffuse radiation falling on the collector.

The other terms have been defined in Chapter 3.

Thus, in order to evaluate q_u in Eq. (4.1), it is necessary to derive expressions for calculating the values of $(\tau\alpha)_b$, $(\tau\alpha)_d$ and q_l. This calculation will therefore be taken up in the sections which follow.

At this stage, it will be worthwhile to define two terms, the instantaneous collection efficiency and stagnation temperature. The *instantaneous collection efficiency* is given by

$$\eta_i = \frac{\text{Useful heat gain}}{\text{Radiation incident on the collector}} = \frac{q_u}{A_p I_T} \tag{4.3}$$

In the definition given in Eq. (4.3), the area of the absorber plate, A_p, is used in the denominator. Often the collector aperture area (A_a) or the collector gross area (A_c) is also used. The *collector aperture area* is the net opening in the topmost cover through which solar radiation is admitted into the collector, while the *collector gross area* is the area of the topmost cover (including the frame). A_a is usually about 10 to 15 per cent more than A_p, while A_c is about 15 to 20 per cent more than A_p.

If the liquid flow rate through the collector is stopped, there is no useful heat gain and the efficiency is zero. In this case, the absorber plate attains a temperature such that $A_p S = q_l$. This temperature is the highest that the absorber plate can attain and is sometimes referred to as the *stagnation temperature*. Knowledge of the stagnation temperature is useful as an indicator for comparing different collector designs. It also helps in choosing proper materials for construction of the collector.

It has been stated earlier (Sec. 3.6.3) that many solar processes occur at a relatively slow pace. As a result, the time base of an hour is often convenient. Thus Eq. (4.3) is also valid as an expression for calculating the hourly collection efficiency, if q_u is the useful heat gain in one hour (kJ/h) and I_T is the energy incident on the collector face in one hour (kJ/m^2-h).

4.3 TRANSMISSIVITY OF THE COVER SYSTEM

The transmissivity of the cover system of a collector can be obtained with adequate accuracy by considering reflection-refraction and absorption separately, and is given by the product form

$$\tau = \tau_r \tau_a \tag{4.4}$$

where τ_r = transmissivity obtained by considering only reflection and refraction

and τ_a = transmissivity obtained by considering only absorption.

4.3.1 Transmissivity Based on Reflection-Refraction

When a beam of light of intensity I_{bn} travelling through a transparent medium 1 strikes the interface separating it from another transparent medium 2, it is reflected and refracted (Fig. 4.1). The reflected beam has reduced intensity I_r and has a direction such that the angle of reflection is equal to the angle of incidence. On the other hand, the directions of the incident and refracted beams are related to each other by Snell's law which states that

$$\frac{\sin \theta_1}{\sin \theta_2} = \frac{n_2}{n_1} \tag{4.5}$$

where θ_1 = angle of incidence,

θ_2 = angle of refraction,

n_1, n_2 = refractive indices of the two media.

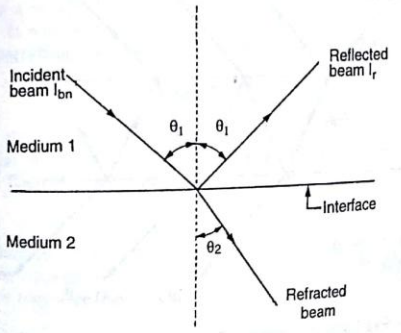

Fig. 4.1 Reflection and Refraction at the Interface of two Media

The reflectivity ρ ($= I_r/I_{bn}$) is related to the angles of incidence and refraction by the equations

$$\rho = \frac{1}{2}(\rho_\perp + \rho_\parallel)$$

$$\rho_\perp = \frac{\sin^2(\theta_2 - \theta_1)}{\sin^2(\theta_2 + \theta_1)} \tag{4.3}$$

$$\rho_\parallel = \frac{\tan^2(\theta_2 - \theta_1)}{\tan^2(\theta_2 + \theta_1)} \tag{4.4}$$

$\rho_\perp$ and $\rho_\parallel$ being the reflectivities of the two components of polarization.

For the special case of normal incidence ($\theta_1 = 0°$), it can be shown that

$$\rho = \rho_\perp = \rho_\parallel = \left(\frac{n_1 - n_2}{n_1 + n_2}\right)^2 \tag{4.5}$$

The transmissivity τ_r is given by an expression similar to that for ρ. Thus

$$\tau_r = \frac{1}{2}(\tau_\perp + \tau_\parallel) \tag{4.6}$$

where $\tau_\perp$ and $\tau_\parallel$ are the transmissivities of the two components of polarization.

Consider one of the components of polarization of a beam incident on a single cover. Because of the fact that there are two interfaces, multiple reflections and refractions will occur as shown in Fig. 4.2.

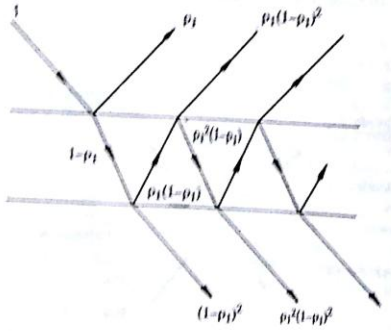

Fig. 4.2 Ray Diagram Showing Transmission Through a Single Cover Considering Reflection-Refraction Alone

$$\tau_\perp = (1-\rho_1)^2 + \rho_1^2(1-\rho_1)^2 + \rho_1^4(1-\rho_1)^2 + \ldots$$

Hence,

$$= (1-\rho_1)^2(1 + \rho_1^2 + \rho_1^4 + \ldots)$$

$$= \frac{(1-\rho_1)^2}{1-\rho_1^2} = \frac{1-\rho_1}{1+\rho_1} \tag{4.10}$$

Similarly,

$$\tau_\parallel = \frac{1-\rho_\parallel}{1+\rho_\parallel} \tag{4.11}$$

These results can be readily extended to a system of M covers for which it can be shown that

$$\tau_\perp = \frac{1-\rho_\perp}{1+(2M-1)\rho_\perp} \tag{4.12}$$

$$\tau_\parallel = \frac{1-\rho_\parallel}{1+(2M-1)\rho_\parallel} \tag{4.13}$$

and

4.3.2 Transmissivity Based on Absorption

The transmissivity based on absorption can be obtained by assuming that the attenuation due to absorption is proportional to the local intensity (Bouger's law). Consider a beam of intensity I_{bn} incident normally on a transparent cover of thickness δ_c and emerging with an intensity I_t (Fig. 4.3). From Bouger's law

$$dI = -KI\,dx$$

where K is a constant of proportionality and is called the *extinction coefficient*. It will be assumed to have a value independent of wavelength. Integrating over the length traversed by the beam, we have

$$\tau_\alpha = \frac{I_t}{I_{bn}} = e^{-K\delta_c} \tag{4.14}$$

In case the beam is incident at an angle θ_1, the path traversed through the cover would be $(\delta_c/\cos\theta_2)$, where θ_2 is the angle of refraction. Then Eq. (4.14) gets modified to the form

$$\tau_\alpha = e^{-K\delta_c/\cos\theta_2} \tag{4.15}$$

The extinction coefficient K is a property of the cover material. Its value varies from about 5 to 25 m^{-1} for different qualities of glass. A low value is obviously desirable.

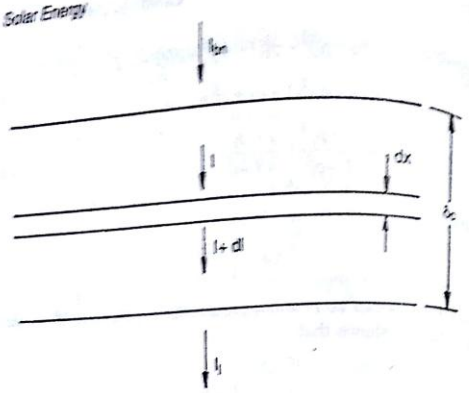

Fig. 4.3 Absorption in a Transparent Cover

Example 4.1

Plot the variation of τ_r, τ_a and τ with the angle of incidence for the following cover system

Material	: Glass
Number of covers	= 3
Thickness of each cover	= 4 mm
Refractive index of glass relative to air	= 1.52
Extinction coefficient of glass	= 15 m^{-1}

- The calculation is given in detail for one angle of incidence, viz. $\theta_1 = 15°$

Hence, $\theta_2 = \sin^{-1}[(\sin 15°)/1.52] = 9.80°$

$$\rho_I = \frac{\sin^2(9.80° - 15°)}{\sin^2(9.80° + 15°)} = 0.047$$

$$\rho_{II} = \frac{\tan^2(9.80° - 15°)}{\tan^2(9.80° + 15°)} = 0.039$$

$$\tau_{rI} = \frac{1 - 0.047}{1 + (5 \times 0.047)} = 0.773$$

$$\tau_{rII} = \frac{1 - 0.039}{1 + (5 \times 0.039)} = 0.805$$

$$\tau_r = \frac{1}{2}(0.773 + 0.805) = 0.789$$

$$\tau_a = \exp[-(3 \times 15 \times 4 \times 10^{-3}/\cos 9.80°)] = 0.833$$

$$\tau = 0.789 \times 0.833 = 0.657$$

The transmissivities for other angles of incidence are obtained in a similar manner. Their variation with the angle of incidence is shown in Fig. 4.4. It will be seen that the values are essentially constant up to angles of incidence of 45°. Thereafter, the values drop rather sharply to zero as the angle of incidence increases to 90°.

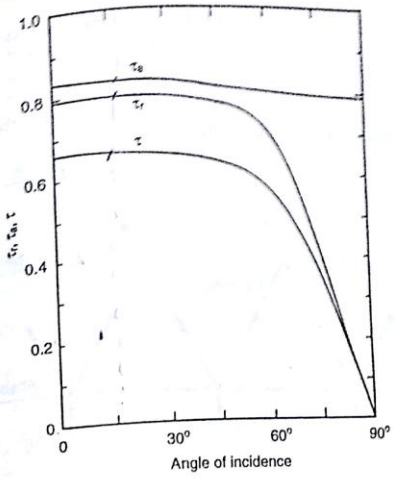

Fig. 4.4 Example 4.1—Variation of τ_r, τ_a and τ with Angle of Incidence

4.3.3 Transmissivity for Diffuse Radiation

The preceding considerations apply only to beam radiation. Calculation of the transmissivity of a cover system when diffuse radiation is incident on it presents some difficulty, because the radiation comes from many directions. The usual practice is to assume that the diffuse radiation is equivalent to beam radiation coming at an angle of incidence of 60°. This angle is arrived at by considering the variation of τ as seen in Fig. 4.4 and by assuming that the amount of diffuse radiation coming from all directions is the same.

4.4 TRANSMISSIVITY-ABSORPTIVITY PRODUCT

The *transmissivity-absorptivity product* is defined as the ratio of the flux absorbed in the absorber plate to the flux incident on the cover system, and is denoted by the symbol $(\tau\alpha)$, an appropriate subscript (b or d) being added to indicate the type of incident radiation. An expression for the transmissivity-absorptivity product will now be derived.

Out of the fraction τ transmitted through the cover system, a part is absorbed and a part reflected diffusely. Out of the reflected part, a portion is transmitted through the cover system and a portion reflected back to the absorber plate. The process of absorption and reflection at the absorber plate surface (Fig. 4.5) goes on indefinitely, the quantities involved being successively smaller.

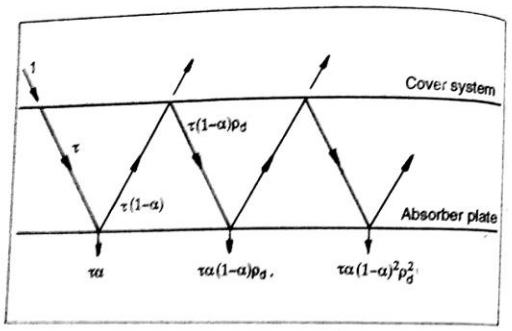

Fig. 4.5 Absorption and Reflection at the Absorber Plate

Thus, the net fraction absorbed $(\tau\alpha)$

$$= \tau\alpha[1 + (1-\alpha)\rho_d + (1-\alpha)^2\rho_d^2 + \ldots]$$

$$= \frac{\tau\alpha}{1-(1-\alpha)\rho_d} \tag{4.16}$$

The symbol ρ_d represents the diffuse reflectivity of the cover system. It can be found by determining the value $\tau_a(1-\tau_r)$ for the cover system for an incidence angle of 60°.

From Example 4.1, it is seen that $\rho_d = 0.24$ for a three glass cover system. Similarly for a one and two glass cover system, the values of ρ_d can be shown to be 0.15 and 0.22 respectively.

4.5 OVERALL LOSS COEFFICIENT AND HEAT TRANSFER CORRELATIONS

It is convenient from the point of view of analysis to express the heat lost from the collector in terms of an overall loss coefficient defined by the equation

$$q_l = U_l A_p(T_{pm} - T_a) \tag{4.17}$$

where U_l = overall loss coefficient,

A_p = area of the absorber plate,

T_{pm} = average temperature of the absorber plate,

and T_a = temperature of the surrounding air (assumed to be the same on all sides of the collector).

The heat lost from the collector is the sum of the heat lost from the top, the bottom and the sides. Thus,

$$q_l = q_t + q_b + q_s$$

where q_t = rate at which heat is lost from the top,

q_b = rate at which heat is lost from the bottom,

and q_s = rate at which heat is lost from the sides.

Each of these losses is also expressed in terms of coefficients called the top loss coefficient, the bottom loss coefficient and the side loss coefficient and defined by the equations

$$q_t = U_t A_p(T_{pm} - T_a) \tag{4.18}$$

$$q_b = U_b A_p(T_{pm} - T_a) \tag{4.19}$$

$$q_s = U_s A_p(T_{pm} - T_a) \tag{4.20}$$

It will be noted that the definition of each of the coefficients is based on the area A_p and the temperature difference $(T_{pm} - T_a)$. This is done for convenience and helps in giving the simple additive equation

$$U_l = U_t + U_b + U_s \tag{4.21}$$

The losses can also be pictured in terms of thermal resistances as shown in Fig. 4.6. The overall loss coefficient is an important parameter since it is a measure of all the losses. Typical values range from 2 to 10 W/m^2-K.

4.5.1 Top Loss Coefficient

The top loss coefficient U_t is evaluated by considering convection and re-radiation losses from the absorber plate in the upward direction. For purposes of calculation, it is assumed that the transparent covers

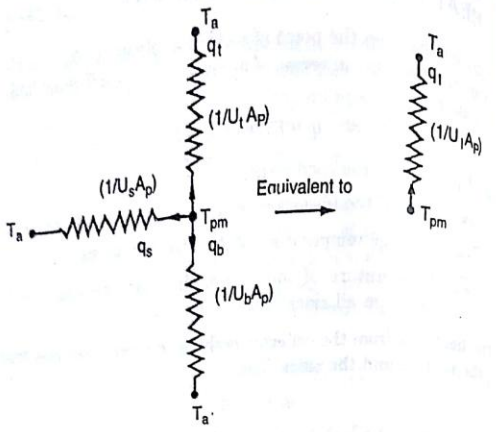

Fig. 4.6 Thermal Resistance Network Showing Collector Losses

and the absorber plate constitute a system of infinite parallel surfaces and that the flow of heat is one-dimensional and steady.* It is further assumed that the temperature drop across the thickness of the covers is negligible and that the interaction between the incoming solar radiation absorbed by the covers and the outgoing loss may be neglected. The outgoing re-radiation is of large wavelengths. For these wavelengths, the transparent cover will be assumed to be opaque. This is a very good assumption if the material is glass.

A schematic diagram for a two-cover system is shown in Fig. 4.7. In a steady state, the heat transferred by convection and radiation between (i) the absorber plate and the first cover, (ii) the first cover and the second cover, and (iii) the second cover and the surroundings must be equal. Hence,

$$\frac{q_t}{A_p} = h_{p-c1}(T_{pm} - T_{c1}) + \frac{\sigma(T_{pm}^4 - T_{c1}^4)}{\left(\frac{1}{\varepsilon_p} + \frac{1}{\varepsilon_c} - 1\right)} \tag{4.22}$$

*H.C. Hottel and B.B. Woertz, "Performance of Flat-Plate Solar-Heat Collectors". *Trans. ASME*, 64, 91 (1942).

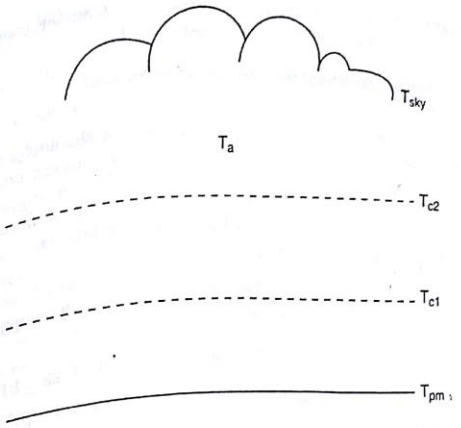

Fig. 4.7 Calculation of the Top Loss Coefficient

$$= h_{c1-c2}(T_{c1} - T_{c2}) + \frac{\sigma(T_{c1}^4 - T_{c2}^4)}{\left(\frac{1}{\varepsilon_c} + \frac{1}{\varepsilon_c} - 1\right)} \tag{4.23}$$

$$= h_w(T_{c2} - T_a) + \sigma\varepsilon_c(T_{c2}^4 - T_{sky}^4) \tag{4.24}$$

where h_{p-c1} = convective heat transfer coefficient between the absorber plate and the first cover,

h_{c1-c2} = convective heat transfer coefficient between the first and second covers,

h_w = convective heat transfer coefficient between the topmost cover (in this case the second) and the surrounding air,

T_{c1}, T_{c2} = temperatures attained by the two covers,

T_{sky} = effective temperature of the sky with which the radiative exchange takes place,

ε_p = emissivity of the absorber plate for long wavelength radiation,

ε_c = emissivity of the covers for long wavelength radiation.

Equations (4.22), (4.23) and (4.24) constitute a set of three non-linear equations which have to be solved for the unknowns q_t, T_{c1} and T_{c2}. However, before this can be done it will be necessary to have some

correlations for calculating the convective heat transfer coefficients h_{p-c}, h_{c-c}, h_{c-g} and h_w, and the sky temperature T_{sky}.

Heat Transfer Coefficient Between Inclined Parallel Surfaces

The natural convection heat transfer coefficient for the enclosed space between the absorber plate and the first cover or between two covers is calculated by using one of the following correlations suggested by Buchberg *et al.*[*] The correlations are based on an examination of available experimental data and all previous correlations.

$$Nu_L = 1; \; Ra_L \cos\beta < 1708$$

$$Nu_L = 1 + 1.446\left(1 - \frac{1708}{Ra_L \cos\beta}\right); \; 1708 < Ra_L \cos\beta < 5900$$

$$Nu_L = 0.229\,(Ra_L \cos\beta)^{0.252}; \; 5900 < Ra_L \cos\beta < 9.23 \times 10^4$$

$$Nu_L = 0.157\,(Ra_L \cos\beta)^{0.285}; \; 9.23 \times 10^4 < Ra_L \cos\beta < 10^6 \quad (4.25)$$

Nu_L and Ra_L are the Nusselt and Rayleigh numbers respectively. The characteristic dimension L is the spacing between the surfaces, while properties are evaluated at the arithmetic mean of the surface temperatures.

Heat Transfer Coefficient at the Top Cover

The convective heat transfer coefficient (h_w) at the top cover has been generally calculated so far, from the following empirical correlation suggested by McAdams,[†]

$$h_w = 5.7 + 3.8V_\infty \quad (4.26)$$

in which h_w is in W/m^2-K and V_∞ is the wind speed in m/s. This correlation is based on the experiments performed by Jurges in 1924 for flow of air at room temperature parallel to a heated vertical plate 0.5 m square. Since the direction of the wind is, in general, not parallel to the top glass cover, it is obvious that Eq. (4.26) suffers from certain limitations.

More recently, Sparrow and his co-workers[‡] have suggested the following dimensionless correlation

[*] H. Buchberg, I. Catton and D.K. Edwards, "Natural Convection in Enclosed Spaces – A Review of Application to Solar Energy Collection", *Journal of Heat Transfer, Trans. ASME*, **98**, 182 (1976).

[†] W.H. McAdams, *Heat Transmission*, 3rd edn., McGraw Hill, New York, p. 249 (1954).

[‡] E.M. Sparrow and W.K. Tien, "Forced Convection Heat Transfer at an Inclined and Forced Square Plate Application to Solar Collectors", *Journal of Heat Transfer, Trans.*

$$j = 0.86\,(Re_{L_c}^*)^{-1/2} \quad (4.27)$$

where j = j-factor given by $(h_w/\rho C_p V_\infty)Pr^{2/3}$

$Re_{L_c}^*$ = Reynolds number $(V_\infty L^*/\nu)$ based on the characteristic dimension $L^* = 4A_c/C_c$

A_c = collector gross area,

C_c = circumference associated with the collector gross area.

Equation (4.27) was recommended on the basis of extensive wind tunnel experiments performed on square and rectangular plates† inclined at various angles of attack and yaw to an on coming air flow. The experiments involved mass transfer with the naphthalene sublimation technique being used for the determination of the mass transfer coefficients. The analogy between heat and mass transfer was used for suggesting the heat transfer correlation.

Comparisons for the same situation show that Eq. (4.26) substantially overestimates the convective loss from the top. Since Eq. (4.27) has been obtained on the basis of extensive data and for more realistic flow situations, it appears desirable to use it in preference to Eq. (4.26). The only short-coming from which it suffers is that it is a forced convection relation. As such, it is likely to underestimate the heat transfer at very low velocities when the natural convection component could be important.

Sky Temperature

The effective temperature of the sky is usually calculated from the following simple empirical relation in which temperatures are expressed in Kelvin.

$$T_{sky} = T_a - 6 \quad (4.28)$$

4.5.2 Bottom Loss Coefficient

The bottom loss coefficient U_b is evaluated by considering conduction and convection losses from the absorber plate in the downward direction through the bottom of the collector. It will be assumed that the flow of heat is one dimensional and steady (Fig. 4.8). In most cases, the thickness of insulation provided is such that the thermal resistance associated with conduction dominates. Thus, neglecting the convective resistance at the bottom surface of the collector casing, we have

† E.M. Sparrow, J.W. Ramsey and E.A. Mass, "Effect of Finite Width on Heat Transfer and Fluid Flow about an Inclined Rectangular Plate", *Journal of Heat Transfer, Trans.*

$$U_b = \frac{k_i}{\delta_b}$$

where k_i = thermal conductivity of the insulation,

δ_b = thickness of the insulation.

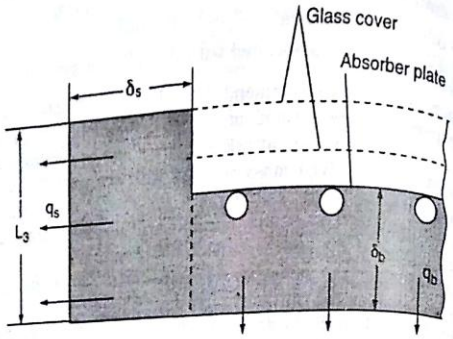

Fig. 4.8 Bottom and Side Losses from a Flat-plate Collector

4.5.3 Side Loss Coefficient

As in the case of the bottom loss coefficient, it will be assumed that the conduction resistance dominates and that the flow of heat is one-dimensional and steady. The one-dimensional approximation can be justified on the grounds that the side loss coefficient is always much smaller than the top loss coefficient.

If the dimensions of the absorber plate are $L_1 \times L_2$ and the height of the collector casing is L_3, then the area across which heat flows sideways is $2(L_1 + L_2)L_3$. The temperature drop across which the heat flow occurs varies from $(T_{pm} - T_a)$ at the absorber plate level to zero both at the top and bottom. Assuming, therefore, that the average temperature drop across the side insulation is $(T_{pm} - T_a)/2$ and that the thickness of this insulation is δ_s, we have

$$q_s = 2L_3(L_1 + L_2)k_i \frac{(T_{pm} - T_a)}{2\delta_s} \tag{4.30}$$

Thus, from Eq. (4.20),

$$U_s = \frac{(L_1 + L_2)L_3 k_i}{L_1 L_2 \delta_s} \tag{4.31}$$

Example 4.2

Calculate the overall loss coefficient for a flat-plate collector with two glass covers with the following data:

Size of absorber plate	= 0.90 m × 1.90 m
Spacing between plate and first glass cover	= 4 cm
Spacing between first and second glass cover	= 4 cm
Plate emissivity	= 0.92
Glass cover emissivity	= 0.88
Collector tilt	= 20°
Mean plate temperature	= 70°C
Ambient air temperature	= 24°C
Wind speed	= 2.5 m/s
Back insulation thickness	= 8 cm
Side insulation thickness	= 4 cm
Thermal conductivity of insulation	= 0.05 W/m-K

From Eq. (4.28),

$$T_{sky} = 297.2 - 6 = 291.2 \text{ K}$$

Substituting this value and the given values of T_{pm}, T_a, ε_p and ε_c in Eqs (4.22) to (4.24), we have

$$\frac{q_t}{A_p} = h_{p-c1}(343.2 - T_{c1}) + \frac{5.67 \times 10^{-8}(343.2^4 - T_{c1}^4)}{\left(\frac{1}{0.92} + \frac{1}{0.88} - 1\right)}$$

$$= h_{p-c1}(343.2 - T_{c1}) + 4.6350 \times 10^{-8}(138.736 \times 10^8 - T_{c1}^4) \tag{4.32}$$

$$\frac{q_t}{A_p} = h_{c1-c2}(T_{c1} - T_{c2}) + \frac{5.67 \times 10^{-8}(T_{c1}^4 - T_{c2}^4)}{\left(\frac{1}{0.88} + \frac{1}{0.88} - 1\right)}$$

$$= h_{c1-c2}(T_{c1} - T_{c2}) + 4.455 \times 10^{-8}(T_{c1}^4 - T_{c2}^4) \tag{4.33}$$

and

$$\frac{q_t}{A_p} = h_w(T_{c2} - 297.2) + 5.67 \times 10^{-8} \times 0.88(T_{c2}^4 - 291.2^4)$$

$$= h_w(T_{c2} - 297.2) + 4.990 \times 10^{-8}(T_{c2}^4 - 71.9061 \times 10^8) \tag{4.34}$$

Equations (4.32) to (4.34) have to be solved for the unknowns (q_t/A_p), T_{c1} and T_{c2}. For this, the values of h_{p-c1}, h_{c1-c2} and h_w are needed. Since these values depend upon T_{c1} and T_{c2}, a trial-and-error method becomes necessary.

Assume $T_{c1} = 325$ K

$T_{c2} = 305$ K

4.6 COLLECTOR EFFICIENCY FACTOR

In Sec. 4.5, procedures for calculating the overall loss coefficient were described. The heat lost from the collector can thus be calculated, if the average plate temperature is known. However, this temperature is generally not known. It will, therefore, be necessary to consider the flow of heat in the absorber plate and across the fluid tubes to the fluid so that the values of T_{pm} can be related to the value of the inlet fluid temperature, which is a known quantity.

In order to simplify the problem, the approach adopted will be to

---

*H.P. Garg and G. Datta, "The Top Loss Calculation for Flat-plate Solar Collectors"

7. *Instantaneous Efficiency*

Using Eq. (4.3), the instantaneous efficiency based on the ab... plate area is given by

$$\eta_i = \frac{560.1}{852.7 \times 1.5}$$

$$= 0.438, \text{ i.e. } 43.8 \text{ per cent.}$$

Considering the fact that the water inlet temperature is only 6... the efficiency of the given collector is rather low. This is so because t... glass covers used are of poor quality and have a low transmissivity... Also the thermal conductivity of the absorber plate material is low... similar collector having a copper or aluminium absorber plate and... fitted with better glass covers having a lower extinction coefficient... would, under comparable conditions, yield a higher efficiency between... 50 and 55 per cent (see problem 7). However, it should be noted that... such a collector would cost more than the GI collector.

Performance Over a Day

It is of interest to study the performance of a collector over a whole... day. This is done for the same GI collector by using radiation data... measured over a whole day. For the sake of simplicity, the water flow... rate, water inlet temperature, ambient temperature and wind speed... are all assumed to be constant at the values given earlier.

The radiation data used and the results obtained are given in Table 4.1... It is seen that the values of the useful heat gain and the efficiency... (Fig. 4.11) increase sharply from 0800 to 1000 h, touch a peak around... noon and then drop sharply after 1500 h. The variation obtained is... typical for a flat-plate collector and indicates the strong dependence of... these factors on the radiation incident on the collector. It is also seen... that the value of the top loss coefficient does not vary much.

Table 4.1 Performance of a Flat-plate Collector Over a Whole Day

IST (h)	0800	0900	1000	1100	1200	1300	1400	1500	1600	1700
I_b (W/m^2)	213	390	547	665	725	715	615	476	337	186
I_d (W/m^2)	149	192	210	230	230	233	239	221	185	141
I_T (W/m^2)	319.2	535.8	712.4	852.7	914.7	908.2	814.8	658.2	482.8	290.9
T_{pm} (K)	334.1	339.6	344.1	347.5	349.1	348.9	346.6	342.9	338.5	333.7
U_t (W/m^2-K)	3.55	3.62	3.66	3.72	3.72	3.72	3.70	3.65	3.60	3.55
q_u (W)	37.1	252.5	427.3	560.1	619.6	613.5	524.6	378.2	209.9	20.8
T_{fo} (K)	333.6	336.3	338.4	340.1	340.8	340.7	339.6	337.8	335.7	333.4
η_i (%)	7.7	31.4	40.0	43.8	45.2	45.0	42.9	38.3	29.0	4.8

The average efficiency over the whole period, during which useful

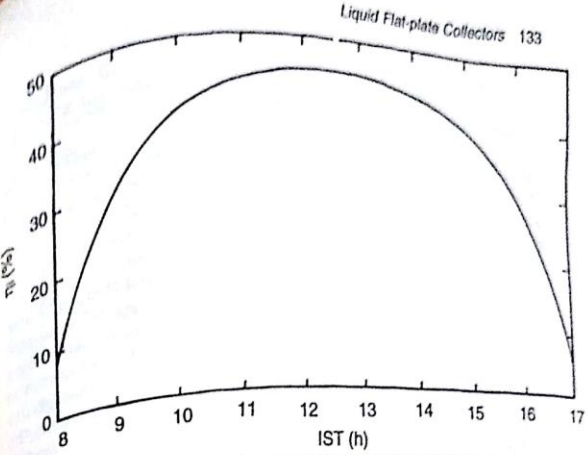

Fig. 4.11 Variation of Instantaneous Efficiency of a GI Collector over a Day (η_i Based on Absorber Plate Area)

energy is collected, can be approximately calculated if it is assumed that the values of instantaneous efficiency and solar radiation are valid for half an hour on either side of the instant considered. Making this approximation, the efficiency averaged over 10 hours from 0730 to 1730 h works out to be 37.4 per cent.

4.9 EFFECTS OF VARIOUS PARAMETERS ON PERFORMANCE

It is evident from the preceding sections and from Example 4.3 that a large number of parameters influence the performance of a liquid flat-plate collector. These parameters could be classified as design parameters, operational parameters, meteorological parameters and environmental parameters. In this section, the effects of some of these will be considered. The parameters discussed are the selectivity of the absorber surface, the number of glass covers, the spacing between the covers, the tilt of the collector, the fluid inlet temperature, the incident solar flux, and dust settlement on the top glass cover.

4.9.1 Selective Surfaces

Absorber plate surfaces which exhibit the characteristics of a high value of absorptivity for incoming solar radiation and a low value of emissivity for out-going re-radiation are called *selective surfaces*. Such surfaces are desirable because they maximize the absorption of solar

energy and minimize the emission of the radiative loss. Obviously it would yield higher collector efficiencies than are obtained when the absorptivity and emissivity are equal.

The possibility of having selective absorber plate surfaces for flat-plate collectors was suggested first by Tabor* and later by Gier and Dunkle†. The basis for the suggestion can be understood if one compares the spectral distribution of extra-terrestrial solar radiation with that of blackbody radiation from a source at 350 K (which corresponds approximately to the temperature of the absorber plate). These are shown in Fig. 4.12 (a) and it is immediately obvious that there is almost no overlap between the two. Unlike solar radiation, which lies almost exclusively in the wavelength region up to 4 μm, the radiation coming off from the absorber plate is of large wavelengths with a maximum at 8.3 μm. It follows therefore that if a surface that has a high absorptivity for wavelengths less than 4 μm and a low emissivity for wavelengths greater that 4 μm can be prepared, it would have the characteristics desirable for an absorber plate surface to act in a selective fashion. The characteristics desired for an ideal selective surface ($\alpha_\lambda = \varepsilon_\lambda = 1$ for $\lambda < 4$ μm and $\alpha_\lambda = \varepsilon_\lambda = 0$ for $\lambda > 4$ μm) are shown in Fig. 4.12 (b). For comparison, the variation obtained for one of the earliest surfaces synthesised by Tabor is also shown.

The development of selective surfaces on various metal substrates has been the subject of intensive work for many years. As a result, a number of surfaces having characteristics approaching those of an ideal surface have been synthesised and a few have been commercialised. In most of these surfaces the selectivity is achieved by having a polished and cleaned metal base and depositing on it a thin surface layer which is transparent to large wavelengths, but highly absorbing for small wavelength solar radiation. The surface layer is less than 1 μm in thickness and is deposited by a variety of methods. These include electroplating, chemical vapour deposition, chemical conversion, anodic oxidation and rf-magetron sputtering. Some of the successful developments in this field will now be described.

Surface layers of copper oxide and "nickel black" were the first selective surfaces found to be suitable from a practical standpoint. The copper oxide layer was formed by chemical conversion, by treating a cleaned and polished copper plate in a hot solution of sodium hydroxide and sodium chlorite for a specified time. Values of absorptivity (α) and emissivity (ε_p) obtained for this surface were 0.89 and 0.17 respectively,

*H. Tabor, "Selective Radiation", *Bulletin Research Council of Israel*, **5A**, 119 (1956).
†J.T. Gier and R.V. Dunkle, "Selective Spectral Characteristics as an Important Factor in the Efficiency of Solar Collectors", *Trans. Conf. on the Use of Solar Energy*, **2**, Part I, 41 (1958).

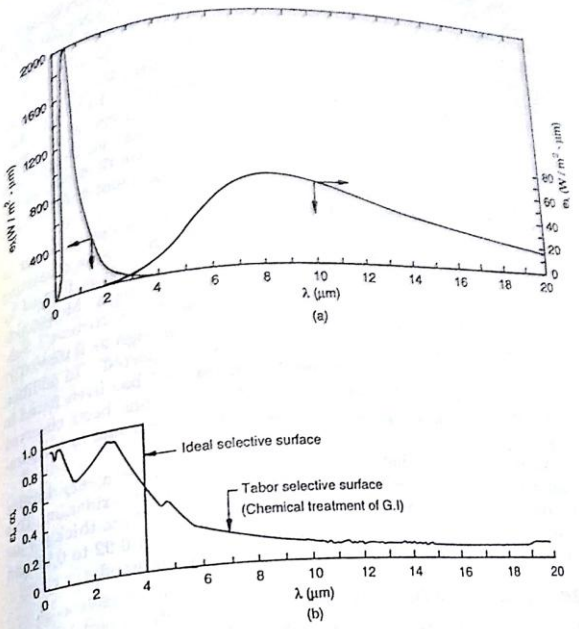

Fig. 4.12 (a) Spectral Distribution of Extra-terrestrial Solar Radiatio and Blackbody Radiation from a Source at 350 K
(b) Monochromatic Emissivity/Absorptivity Variation Desire for an Ideal Selective Surface and Variation Obtained for Selective Surface by Tabor

α being the average value of α_λ over the solar radiation waveleng range and ε_p being the average value of ε_λ for large waveleng radiation. This surface was commercialised in Australia* and found be durable for low temperature applications like solar water heatin

*D.J. Close, "Flat Plate Solar Absorbers: The Production and Testing of a Select Surface for Copper Absorber Plates", *Report E.D. 7, C.S.I.R.O.*, Melbourne, Austr (1962).

The "nickel black" surface was developed and commercialised in Israel*. The process involved the careful cleaning of a galvanised iron sheet and subsequent electroplating of a "nickel black" coating by immersion of the sheet as the cathode in an aqueous electrolytic bath of nickel sulphate, zinc sulphate, ammonium sulphate, ammonium thiocyanate and citric acid. Values of $\alpha = 0.81$ and $\varepsilon_p = 0.16$ to 0.1[illegible] obtained for this selective surface. Subsequently Cathro et al.† described procedures for electroplating "nickel black" on copper and mild steel. In these cases, a bright nickel plating was first put on the base metal before electroplating "nickel black". Values of $\alpha = 0.9$[illegible] $\varepsilon_p = 0.09$ to 0.15 were reported.

One of the most successful selective surfaces developed so far is "black chrome". This coating is a metal-dielectric composite consisting of a Cr_2O_3 layer over a Cr particle/Cr_2O_3 composite. It is formed by electroplating on a nickel plated copper or steel base. McDonald‡ reported values of $\alpha = 0.868$ and $\varepsilon_p = 0.088$ for "black chrome". Subsequently with further refinements, values of α as high as 0.92 to 0.9[illegible] and values of ε_p as low as 0.04 to 0.06 have been reported.+ In addition to its excellent selective properties, "black chrome" has been found to be very durable. No degradation in performance has been observed even after prolonged exposure to a humid atmosphere and to temperatures up to 400°C.

Andersson *et al.*++ have reported the development of a very durable metal-dielectric composite coating formed by anodic oxidation. This coating consists of grains of nickel embedded in a 0.7 μm thick porous layer of Al_2O_3. Values of absorptivity in the range of 0.92 to 0.97 and emissivity in the range of 0.1 to 0.26 have been obtained.

Effect on Collector Performance

The effect of a selective surface on the performance of a collector can be best illustrated by taking a specific situation. The GI collector of

*H. Tabor, J. Harris, H. Weinberger and B. Doron, "Further Studies on Selective Black Coatings", *Proceedings U.N. Conference on New Sources of Energy*, 4, 618 (1964).

†K.J. Cathro, E.A. Christie and A.F. Reid, "Nickel Black as a Selective Absorbing Surface", Meeting on Applications of Solar Energy Research and Development in Australia, Melbourne (1975).

‡G.E. McDonald, "Spectral Reflective Properties of Black Chrome for Use as a Solar Selective Coating", *Solar Energy*, 17, 119 (1975).

+R.R. Sowell and D.M. Mattox, "Properties and Composition of Electroplated Black Chrome", Symposium on Coatings for Solar Collectors, American Electroplaters Society, Winter Park, Florida, USA (1976).

++A. Andersson, O. Hunderi and C.G. Granqvist, "Nickel Pigmented Anodic Aluminium Oxide for Selective Absorption of Solar Energy", *Journal of Applied Physics*, 51, 754 (1980).

Sec. 4.8 is considered again and its performance with and without a selective surface at 1200 h (IST) calculated. The only changes made from the earlier data are as follows:

(1) It is assumed now that the tubes are clamped on the underside of the absorber plate instead of being brazed. This is a cheaper method of fabrication but results in a bond resistance which is assumed to be 0.15 m-°C/W in this case.

(2) The mean flow rate is taken as 60 kg/h.

(3) The ambient air temperature is assumed to be 30°C.

(4) With the selective surface, two cases are considered. In one case, it is assumed that $\alpha = 0.95$ and $\varepsilon_p = 0.12$, while in the other, it is assumed that $\alpha = 0.85$ and $\varepsilon_p = 0.11$.

The calculations are repeated in a manner similar to that adopted earlier and the results obtained are indicated in Table 4.2.

Table 4.2 Effect of a Selective Surface on Performance of GI Collector

	Nonselective absorber plate $\alpha = \varepsilon_p = 0.95$	Selective absorber plate	
		$\alpha = 0.95$, $\varepsilon_p = 0.12$	$\alpha = 0.85$, $\varepsilon_p = 0.11$
T_{pm} (K)	356.1	359.3	357.0
U_t (W/m²-K)	3.87	2.56	2.51
q_u (W)	593.6	682.9	616.1
T_{fo} (K)	341.7	342.95	342.0
η_i (%)	43.3	49.8	44.9

It is seen from Table 4.2 that with a nonselective absorber plate, the top loss coefficient is 3.87 W/m²-K and the efficiency is 43.3 per cent. These values are similar to those given in Table 4.1, where $U_t = 3.72$ W/m²-K and $\eta_i = 45.2$ per cent. The differences are due to the changes (1) to (3). On the other hand, with the first selective surface, in which the value of α is unchanged while the value of ε_p is 0.12, significant differences are observed. The top loss coefficient drops to 2.56 W/m²-K, while the efficiency increases by 6.6 per cent to 49.8 per cent. With the second selective surface, in which the value of α is much less, it is observed that while the value of U_t is the same as that for the first selective surface, the efficiency is much lower and almost the same as for the non-selective surface. This is primarily due to the fact that the value of S decreases with lower α. It is to be noted that for both the selective surfaces, the value of (α/ε_p) is almost the same. For the first, it is 7.9 and for the second 7.7. This shows that a high value of (α/ε_p) is not adequate for obtaining a good performance with a selective surface. Along with the high value of (α/ε_p), it is necessary that the value of α should also be high.

4.9.2 Number of Covers

The number of covers (glazings) used in a collector is usually one or two. We will study the effect of the number of covers on performance by again taking the example of the GI collector with one, two and three covers. It is assumed that the changes (1) to (3) indicated in Sec. 4.9.1 are again made.

The results obtained are given in Table 4.3 and show that for the situation studied the efficiency goes through a maximum value of 43.3 per cent for the case of two covers. This can be explained as follows.

As the number of covers increases, the values of both $(\tau\alpha)_b$ and $(\tau\alpha)_d$ decrease. Thus, the flux S absorbed in the absorber plate decreases. The addition of more covers also causes the value of U_t, and hence the heat loss, to decrease. However, the amount of decrease is not the same in both cases. For this reason, the efficiency goes through a maximum. This kind of result is obtained with all collectors, the maximum efficiency being usually obtained with one or two covers. In fact, for the GI collector under study, the efficiency will be found to be a maximum with only one cover if a selective absorber surface is used. This is seen from Table 4.4.

Table 4.3 Effect of Number of Covers on Performance of GI Collector (Non-selective Surface)

	Number of covers		
	1	2	3
$(\tau\alpha)_b$	0.8316	0.7305	0.6447
$(\tau\alpha)_d$	0.7567	0.6424	0.5631
U_t (W/m^2-K)	6.39	3.87	2.72
η_i (%)	40.6	43.3	41.8

Table 4.4 Effect of Number of Covers on Performance of GI Collector (Selective Surface, $\alpha = 0.85$, $\varepsilon_p = 0.11$)

	Number of covers	
	1	2
$(\tau\alpha)_b$	0.7563	0.6999
$(\tau\alpha)_d$	0.6882	0.5891
U_t (W/m^2-K)	3.61	2.51
η_i (%)	47.0	44.9

4.9.3 Spacing

The proper spacing to be kept between the absorber plate and the first cover, or between two covers has been the subject of considerable discussion. From the point of view of the heat loss from the top, it is evident that the spacing must be such that the values of the convective heat transfer coefficients are minimized. It is, therefore, useful to examine the behaviour of the correlating equations (4.25). This is done in Fig. 4.13 in which the variation of the heat transfer coefficient with spacing is drawn. Curves for two temperature differences are plotted with the mean air temperature and the tilt being kept fixed.

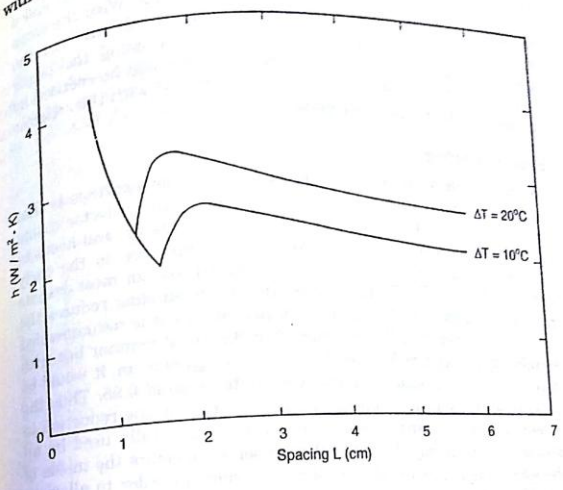

Fig. 4.13 Plot of Eq. 4.25 Showing Variation of Heat Transfer Coefficient with Spacing. $T_{mean} = 70°C$, $\beta = 20°$

It is seen that for a particular temperature difference, the value of h first decreases and reaches a minimum. This variation corresponds to the conduction regime in which $Nu_L = 1$, with the minimum occurring at a spacing corresponding to $Ra_L \cos\beta = 1708$. Thereafter, as the spacing increases the value of h increases first sharply and then gradually. It goes through a maximum and then gradually decreases. With large values of spacing, the value drops below the previous minimum value.

It will be noted that the spacings at which the minimum and maximum values occur vary with the temperature difference. They

also vary with the tilt. Since collectors are designed to operate in different locations with varying tilts and under varying service conditions, an optimum value of spacing is difficult to specify. It appears best to use a sufficiently large spacing away from the local minimum and maximum. Spacings from 4 to 8 cm have been suggested from this point of view by Buchberg *et al.*

Buchberg *et al.* have also studied the effect of spacing on the performance of a collector. They have done calculations for a single and double cover collector with a non-selective absorber plate and a single cover collector with a selective absorber plate. With the same operating conditions, two spacings have been tried out and the efficiency calculated. It has been shown that by using the larger spacing, around 5 cm, collector area requirements can be reduced by 2 to 8 per cent, the higher reduction being obtained with the collector having the selective absorber plate.*

Effect of Shading

The main problem associated with the use of larger spacings is that shading of the absorber plate by the side walls of the collector casing increases. Some shading always occurs in every collector and needs to be corrected for. The shading is particularly important in the early morning and late evening hours. It is estimated that for most designs using spacings of 2 to 3 cm between the covers, shading reduces the radiation absorbed by about 3 per cent. Accordingly, it is recommended that the absorbed flux S be calculated in the usual manner but with a multiplying factor of 0.97. With larger spacings of 5 cm, it would be necessary to use a smaller multiplying factor around 0.95. Thus the gain obtained by using a larger spacing is offset by the reduction in S. For this reason, spacings of 2 or 3 cm are generally used by all manufacturers. It may be noted that in some collectors the inside of the side walls is lined with a reflecting surface in order to alleviate the effects of shading.

4.9.4 Collector Tilt

Flat-plate collectors are normally fixed in one position and do not track the sun. The question of the amount of tilt one should give to them is therefore of considerable importance. The basis for arriving at an optimum tilt will now be discussed.

One of the earliest studies on the subject is due to Morse and Czarnecki* who simplified the problem by assuming that extra-terrestrial insolation was falling on the collector. They calculated the annual insolation per unit area by integrating the expression for the flux on a tilted surface first over the day length and then summing up over the days of the year. Taking $\gamma = 0$, so that the daily insolation is maximized, the following expression is obtained

$$\text{Annual Insolation} = \sum_{n=1}^{365} I_{sc} \int_{-\omega_s}^{+\omega_s} \left(1 + 0.033 \cos \frac{360n}{365}\right) \times (\sin \delta \sin \overline{\phi - \beta} + \cos \delta \cos \omega \cos \overline{\phi - \beta}) d\omega$$

They have plotted their results in the form of relative insolation (the ratio of annual insolation for given values of ϕ and β to the annual insolation for $\phi = 0$ and $\beta = 0$) against the latitude ϕ for tilts of 0, 0.9ϕ, 1.2ϕ and 1.5ϕ. The results are shown in Fig. 4.14 and indicate

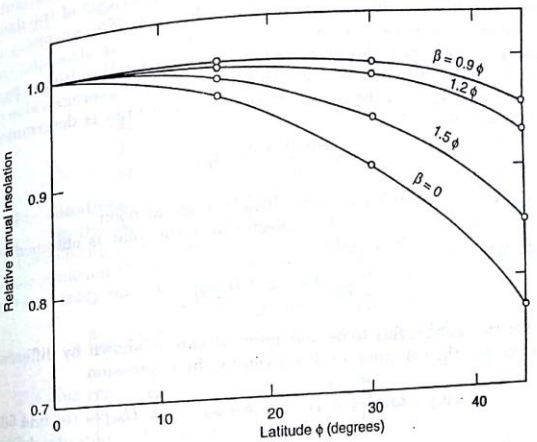

Fig. 4.14 Variation of Relative Annual Insolation with Latitude for Collectors Tilted at Various Values of β and with $\gamma = 0°$

*H. Buchberg, I. Catton and D.K. Edwards, "Natural Convection in Enclosed Spaces--A Review of Application to Solar Energy Collection", *Journal of Heat Transfer, Trans. ASME*, **98**, 182 (1976).

*R.N. Morse and J.T. Czarnecki, "Flat-plate Solar Absorbers: The Effect on Incident Radiation of Inclination and Orientation", *Report E.E.6, Mechanical Engineering Division, C.S.I.R.O.*, Melbourne (1958).

4.12 TESTING PROCEDURES

Finally we will describe certain standard procedures for the testing of collectors. Standardised testing and rating procedures provide equitable basis for comparing the efficiency of different types of collectors and an essential basis for design and selection of systems. The procedure described here has been widely used and was originally proposed by the National Bureau of Standards (NBS) and the American Society of Heating, Refrigerating, and Air-conditioning Engineers (ASHRAE).* Essential details are also given in a paper by Hill and Streed.† Recently, this procedure has also been adopted in the Indian Standard IS 12933 (Part 5).‡

A schematic diagram showing the essential features of the test set-up is shown in Fig. 4.18. It is a closed loop consisting of the flat-plate collector under test, a liquid pump, a heat exchanger, and a storage tank with an electric immersion heater. A bypass is provided around the pump so that the mass flow rate can be adjusted to the prescribed value. The purpose of the heat exchanger is to remove heat. Thus the combination of the heat exchanger and the storage tank (with the electric immersion heater) provide a means for adjusting and controlling the inlet fluid temperature to the collector to a desired value.

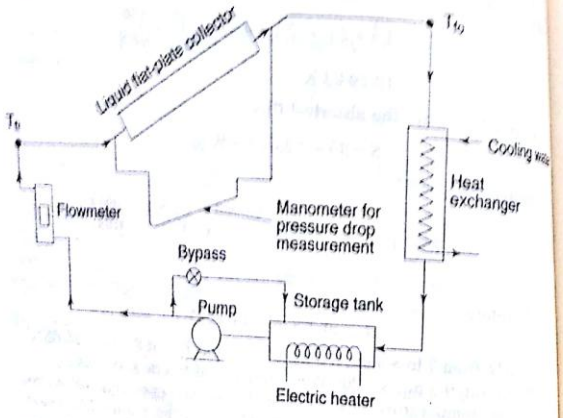

Fig. 4.18 Schematic Diagram of Set-up for Testing Liquid Flat-plate Collectors

The standard specifies that the collector shall be tested under clear sky conditions in order to determine its efficiency characteristics. On any given day, data is recorded under steady state conditions for fixed values of $\dot{m}$ and T_{fi}. For each set of fixed values, it is recommended that an equal number of tests be conducted symmetrically before and after solar noon. Thus, for example, if data of four tests are recorded, these could be at 1100, 1130, 1230 and 1300 h (LAT). In this way, any bias because of transient effects is eliminated. If such data is recorded for four inlet temperatures on different days, then a total of 16 data sets are obtained. This is the minimum number recommended.

The principal measurements made in each data set are the fluid flow rate ($\dot{m}$), the fluid inlet and outlet temperatures of the collector (T_{fi} and T_{fo}), the solar radiation incident on the collector plane (I_T), the ambient temperature (T_a), the pressure drop across the collector (Δp), and the wind speed (V_∞). The efficiency is calculated from the equation

$$\eta_i = \frac{q_u}{A_c I_T} = \frac{\dot{m} C_p (T_{fo} - T_{fi})}{A_c I_T} \tag{4.64}$$

As stated earlier, readings are recorded under steady state conditions. A collector is considered to be operating under steady state conditions if the deviation of the experimental parameters is less than the following specified limits over a 15 minute period:

- Global radiation incident on collector plane ± 50 W/m^2
- Ambient temperature ± 1°C
- Fluid flow rate ± 1 %
- Fluid inlet temperature ± 0.1°C
- Temperature rise across collector ± 0.1°C

In addition, it is specified that the value of I_T should be greater than 600 W/m^2, the wind speed should be between 3 and 6 m/s, and the fluid flow rate should be set at approximately 0.02 kg/s per square metre of collector gross area. It is to be noted that although the procedure suggested is for outdoor testing, it is also applicable for indoor testing with a solar simulator.

The efficiency values calculated from Eq. (4.64) are plotted against the parameter $(T_{fi} - T_a)/I_T$. The reason for doing this is apparent if one considers the Hottel-Whillier-Bliss equation. Dividing both sides of Eq. (4.48) by $A_c I_T$, we have

*ASHRAE Standard 93–77, "Method of Testing to Determine Thermal Performance of Solar Collectors" (1977).

†J.E. Hill and E.R. Streed, "A Method of Testing for Rating Solar Collectors Based on Thermal Performance", *Solar Energy*, 18, 421 (1976).

‡Solar Flat Plate Collector-specification, Part 5—Test Methods, Indian Standard 12933 (Part 5): 1992, Bureau of Indian Standards (1992).

$$\eta_i = F_R\left(\frac{A_p}{A_c}\right)\left[\frac{S}{I_T} - U_l\frac{(T_{fi} - T_a)}{I_T}\right] \tag{4.66}$$

We put

$$S = I_T(\tau\alpha)_{av} \tag{4.67}$$

where $(\tau\alpha)_{av}$ is an average transmissivity-absorptivity product for both beam and diffuse radiation. Hence

$$\eta_i = F_R\frac{A_p}{A_c}\left[(\tau\alpha)_{av} - U_l\frac{(T_{fi} - T_a)}{I_T}\right] \tag{4.67}$$

Since the values of F_R, $(\tau\alpha)_{av}$ and U_l are essentially constant, it is seen from Eq. (4.67) that if η_i is plotted against $(T_{fi} - T_a)/I_T$ a straight line with a negative slope would be obtained. The intercept on the y-axis would give the value of $[F_R(\tau\alpha)_{av}A_p/A_c]$, while the slope of the line would give the value of $[F_RU_lA_p/A_c]$.

In Eq. (4.64), the value of η_i is based on the collector gross area. It could be based on the absorber plate area also. In that case, the term (A_p/A_c) would drop out of Eqs (4.65) and (4.67). The intercept on the y-axis would then be $F_R(\tau\alpha)_{av}$ and the slope of the line would be F_RU_l.

Experimental values of η_i plotted against the parameter $(T_{fi} - T_a)/I_T$ generally yield straight lines. However, the scatter of the data is always large. A typical set of results obtained by testing a commercially available, conventional collector in the Heat Transfer Laboratory at I.I.T. Bombay is shown in Fig. 4.19. A straight line fitted to the data by the method of least squares has the following equation*

$$\eta_i = 0.572 - 4.796(T_{fi} - T_a)/I_T \tag{4.68}$$

For the given collector, $A_p/A_c = 0.848$.

Thus $$F_R(\tau\alpha)_{av} = (0.572/0.848) = 0.675$$

and $$F_RU_l = 4.796/0.848 = 5.656\ \text{W/m}^2\text{-K}$$

It is to be noted that for liquid flat-plate collectors, changes in mass flow rate do not appreciably affect the performance because of the relatively high value of the liquid side heat transfer coefficient h_f. For this reason, although the efficiency curve of a collector is determined for a particular value of mass flow rate, it can also be used for predicting the behaviour of the collector for other flow rates which differ a little from the value used during testing.

It may also be noted that the practice followed in Europe is to plot

*The efficiency values obtained are a little lower than what one might expect from a good quality collector of this type.

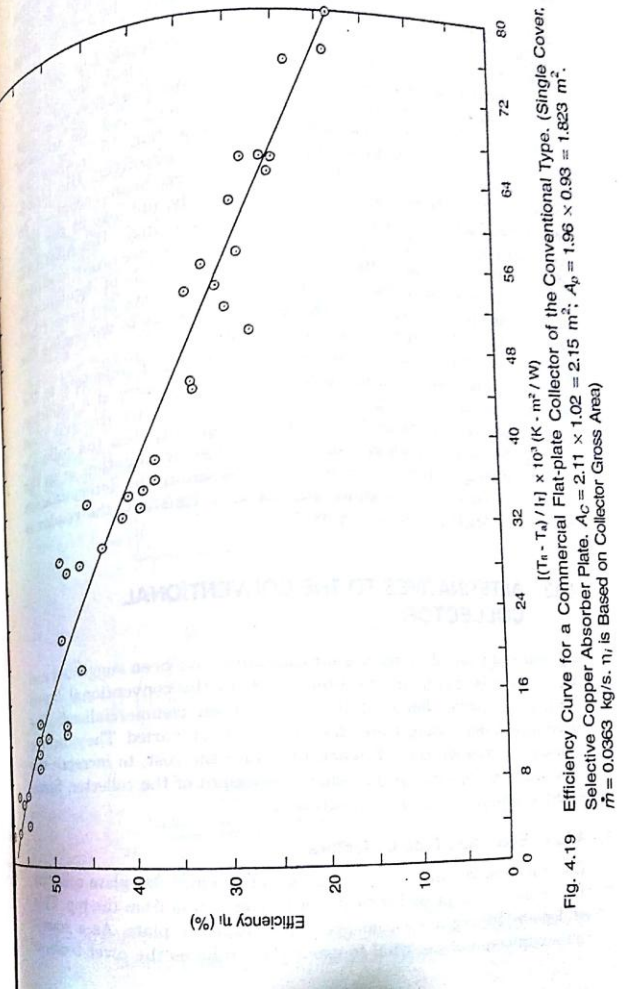

Fig. 4.19 Efficiency Curve for a Commercial Flat-plate Collector of the Conventional Type. (Single Cover, Selective Copper Absorber Plate, $A_C = 2.11 \times 1.02 = 2.15\ m^2$; $A_p = 1.96 \times 0.93 = 1.823\ m^2$; $\dot{m} = 0.0363$ kg/s. η_i is Based on Collector Gross Area)

the efficiency values against the parameter $(\bar{T}_f - T_a)/I_T$, where $\bar{T}_f$ is the arithmetic mean of the liquid inlet and outlet temperatures. In this case also a straight line is obtained, the intercept on the y-axis being $[F'(\tau\alpha)_{av}A_p/A_c]$ and the slope being $(F'U_lA_p/A_c)$.

The standard procedure described for determining the collector efficiency requires that the tests be conducted on a clear day, close to solar noon, so that the value of I_T would be greater than 600 W/m². As a result the beam radiation component is dominant and the angle of incidence of the beam radiation is small (less than 15°). Thus the $(\tau\alpha)_{av}$ term in the parameter $[F_R(\tau\alpha)_{av}A_p/A_c]$ is effectively the transmissivity-absorptivity product for normal incidence beam radiation. In order to characterise collector performance early and late in the day, when the angle of incidence of beam radiation is high, the ASHRAE Standard 93–77 defines a term called the *incidence angle modifier* $K_{\tau\alpha}$ which is the ratio of the $(\tau\alpha)$ product at any angle of incidence to the $(\tau\alpha)$ product at normal incidence. Additional tests are prescribed to be conducted at angles of incidence up to 60° so as to determine the dependence of $K_{\tau\alpha}$ on the angle of incidence.

One more parameter of interest in the testing of collectors is the *time constant*, which is a measure of the heat capacity of a collector. The time constant is defined as the time required for the exit fluid temperature T_{fo} to change by a prescribed amount when the collector is subjected to a step change in the incident solar radiation or in the inlet fluid temperature. For more details regarding the determination of the incidence angle modifier and the time constant, the reader is referred to ASHRAE Standard 93–77.

4.13 ALTERNATIVES TO THE CONVENTIONAL COLLECTOR

A number of novel designs of solar collectors have been suggested and developed over the years as alternatives to the conventional liquid flat-plate collector. Some of these have been commercialised. The objectives in developing these designs have been varied. They include a desire to improve the efficiency, to reduce the cost, to increase the operating temperature, or to reduce the weight of the collector. Some of these designs will now be described.

4.13.1 Evacuated Tube Collectors

One way of improving the performance of a liquid flat-plate collector is to reduce or suppress the heat lost by convection from the top. This is done by having a vacuum above the absorber plate. As a consequence, it becomes essential to use a glass tube as the cover because only a tubular surface is able to withstand the stresses introduced by the pressure difference.

A number of evacuated tube collector (ETC) designs have been developed. One design consists of a number of long cylindrical flat-plate collector modules side-by-side. Each module (Fig. 4.20a) has a metal absorber plate with two fluid tubes housed in an evacuated, cylindrical glass tube. The absorber plate has a selective surface coating on it. Glass-to-metal seals are provided between the fluid tubes and the end cover of the glass tube. From the point of view of thermal stresses, it is necessary to have these at one end. For this reason, the two tubes are joined at the other end inside the glass cover and form a 'U', with one tube acting as the inlet tube and the other as the outlet tube.

A second design is shown in Fig. 4.20b. Here each module consists of three concentric tubes with the space between the outer two tubes, which are made from glass, being evacuated. The outer surface of the middle tube acts as the absorbing surface and has a selective surface coating on it. The liquid flows in through the innermost metal tube and flows out through the annulus between this tube and the middle tube.

In a third design (Fig. 4.20c), the U tube of Fig. 4.20a is replaced by a heat pipe. The length of the heat pipe inside the evacuated glass tube constitutes the evaporator section in which heat is absorbed and the fluid inside the heat pipe evaporates. The evaporated fluid rises to the condenser section where it condenses. The heat of condensation

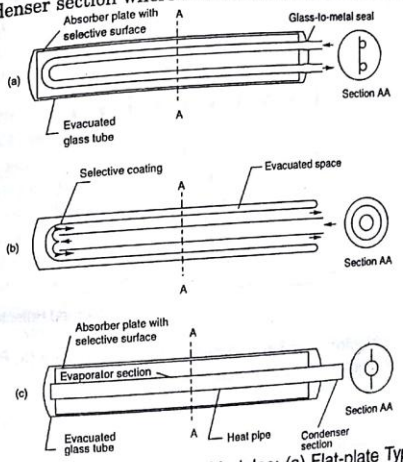

Fig. 4.20 Various Designs of ETC Modules: (a) Flat-plate Type (b) Concentric Tube Type (c) Flat-plate Type with Heat Pipe